Data-Driven Controller Design for Atomic-Force Microscopy

Christoph Kammer * **Adrian P. Nievergelt** **
Georg E. Fantner ** **Alireza Karimi** *

* *Automatic Control Laboratory*
(e-mail: christoph.kammer@epfl.ch, alireza.karimi@epfl.ch)
** *Laboratory for Bio- and Nano-Instrumentation*
(e-mail: adrian.nievergelt@epfl.ch, georg.fantner@epfl.ch)
Ecole Polytechnique Fédérale de Lausanne (EPFL), Switzerland

Abstract: A novel method to design data-driven, fixed-structure controllers with H_2 and H_∞ performance objectives is presented. The control design problem is transformed into a convex optimization problem with linear matrix inequality constraints, which can be solved efficiently with standard solvers. The method is used to design a data-driven controller for an atomic-force microscope. The closed-loop performance of the calculated controller is validated on a real setup.

Keywords: Data-based control, Robust control, Convex optimization, Micro and Nano Mechatronic Systems

1. INTRODUCTION

While the use of measured data for controller tuning is not new, recent advances in the fields of numerical optimization and computational power open up new possibilities for data-driven control design approaches. In these approaches, the controller parameters are directly computed by minimizing a control criterion which is a function of measured data. Therefore, a parametric model of the plant is not required and there are no unmodeled dynamics. The only source of uncertainty is the measurement noise, whose influence can be reduced significantly if the amount of measurement data is large.

Frequency-domain data is used in classical loop-shaping methods for computing simple lead-lag or PID controllers for SISO stable plants. The Quantitative Feedback Theory (QFT) also uses the frequency response of a system to compute robust controllers. New optimization based algorithms have been proposed recently Mercader et al. (2016) to compute QFT controllers. The set of all stabilizing PID controllers with H_∞ performance is obtained using only the frequency-domain data in Keel and Bhattacharyya (2008). This method is extended to design fixed-order linearly parametrized controllers in Parastvand and Khosrowjerdi (2015, 2016). Several data-driven approaches based on frequency-domain data using convex optimization methods have been proposed. A linear programming approach is used to compute linearly parametrized (LP) controllers for SISO systems with specifications in gain and phase margin as well as the desired closed-loop bandwidth in Karimi et al. (2007); Saeki (2014). A convex optimization approach is used to design LP controllers with loop shaping and H_∞ performance in Karimi and Galdos (2010). Recently, the necessary and sufficient conditions for the existence of H_∞ controllers for SISO systems described by their frequency response have been given in Karimi et al. (2016). The use of the frequency response for computing SISO-PID controllers by convex optimization is proposed in Hast et al. (2013). This method uses the same type of linearization of the constraints as Karimi and Galdos (2010), but interprets it as a convex-concave approximation technique. An extension of Hast et al. (2013) for the design of MIMO-PID controllers by linearization of quadratic matrix inequalities is proposed in Boyd et al. (2016) for stable plants. A similar approach is used in Saeki et al. (2010) for designing LP-MIMO controllers (which include PID controllers as a special case). This approach is not limited to stable plants and includes the conditions for the stability of the closed-loop system.

In this paper, a new data-driven controller design approach is presented based on the frequency response and convex optimization. Contrarily to the existing results in Galdos et al. (2010); Boyd et al. (2016); Saeki et al. (2010), the controller is fully parametrized and the design is not restricted to LP or PID controllers. The other contribution is that the approach is not limited to H_∞ performance, but is able to also treat H_2 performance and loop-shaping objectives. The approach also contains a new closed-loop stability proof based on the Nyquist stability criterion. The method is then used to design a controller for an atomic-force microscope (AFM). The superimposed structural resonances of piezo-actuator-based scanners for AFM make high-speed control challenging. Several model-based approaches have been presented over the years in Schitter et al. (2003); Fantner et al. (2006); Ando (2008). However, in practice the use of parametric models has significant disadvantages. The dynamics of the system are of high order, depend on various environmental factors and change often, thus necessitating frequent re-identification between or even during measurements. As the imaging quality in AFM depends on fast, accurate tracking of features, a low

robustness margin is often necessary, which can easily lead to instability due to unmodeled dynamics.

An advantage of data-driven approaches is that frequency response data for AFMs is easily obtainable by identifying the system directly, using the cantilever as a fast and precise sensor. The high positioning speed of the scanner makes it possible to record a large amount of data within short amounts of time, which drastically decreases the influence of measurement noise on the identified response. The authors of Nievergelt et al. (2015) present an approach where filters are tuned manually based on sweep frequency response data to achieve a desired closed-loop bandwidth. Feed-forward compensation by grey-box modeling and subsequent constrained local optimization on sweep frequency response data has been shown to be able to significantly increase the open-loop bandwidth of AFM. However, this process is time-consuming and requires manual interaction while giving no guarantee for robustness or stability. The presented approach is able to design a controller within a short amount of time and to the desired frequency-domain specifications, while also guaranteeing closed-loop stability.

2. PROBLEM FORMULATION

The presented controller design method is equally applicable to both SISO and MIMO cases. For this application, we only present the SISO, discrete-time formulation. A more complete treatment of the theoretical part can be found in Karimi and Kammer (2016).

2.1 Frequency response data

The system to be controlled is a Linear Time-Invariant single-input single-output (LTI-SISO) strictly proper system represented by its frequency response $G(e^{j\omega})$. The frequency response data can easily be obtained using the Fourier analysis method from a set of measurements. We assume that $G(e^{j\omega})$ is bounded in all frequencies except for a set B_g including a finite number of frequencies that correspond to the poles of G on the unit circle. As the frequency function $G(e^{j\omega})$ is periodic, we consider $\omega \in \Omega_g$, where:

$$\Omega_g = \left\{ \omega \,\middle|\, -\frac{\pi}{T_s} \leq \omega \leq \frac{\pi}{T_s} \right\} \backslash B_g \tag{1}$$

and T_s is the sampling period.

2.2 Controller Structure

A fixed-order rational transfer function controller is considered. The controller is defined as:

$$K = X(z)Y(z)^{-1} \tag{2}$$

where:

$$X(z) = (x_p z^p + \cdots + x_1 z + x_0)F_x(z) \tag{3}$$
$$Y(z) = (z^p + \cdots + y_1 z + y_0)F_y(z) \tag{4}$$

with $x_i, y_i \in \mathbb{R}$. The polynomials $F_x(z), F_y(z)$ represent the fixed known terms in the controller, e.g. terms based on the internal model principle or integrators. The set of frequencies of all roots of $F_y(z)$ on the unit circle is denoted by B_y. Note that $Y^{-1}(e^{j\omega})$ should be bounded for all $\omega \in \Omega = \Omega_g \backslash B_y$. This control structure is very general and is not restricted to linearly parameterized controllers.

2.3 Control performance

The control performance is defined as the constraints on the norm of weighted sensitivity functions. A very typical performance specification for reference tracking or disturbance rejection can be defined as:

$$\|W_1 S\| < 1 \tag{5}$$

where $S = (1+GK)^{-1}$ is the sensitivity function, W_1 is the performance weight and $\|\cdot\|$ can be the 2- or infinity-norm. For a stable system $H(z)$, the two- and the infinity-norm are defined as:

$$\|H\|_2^2 = \frac{1}{2\pi} \int_{-\pi/T_s}^{\pi/T_s} H^*(e^{j\omega}) H(e^{j\omega}) d\omega \tag{6}$$

$$\|H\|_\infty = \sup_\omega |H(e^{j\omega})| \tag{7}$$

where $(\cdot)^*$ denotes the complex conjugate. Note that reversely the boundedness of the spectral norms of H does not guarantee the stability of H.

The shape of the open-loop transfer function can also be considered as a form of control performance. In this case, the 2- or infinity-norm of $(L - L_d)$ is minimized, where $L = GK$ and L_d is a desired open-loop transfer function.

3. CONVEX APPROXIMATION

In this section, we show how the performance specifications can be achieved through convex optimization using only the frequency response data of the plant. The performance constraints are represented by a set of convex-concave constraints and then approximated by an inner convex approximation based on the linearization of the concave parts.

3.1 H_∞ performance

Constraints on the infinity-norm of any weighted sensitivity function can be considered. For example, consider the following constraint:

$$\|W_2 T\|_\infty < 1 \tag{8}$$

where $T = GK(I+GK)^{-1}$ is the complementary sensitivity function. This constraint is satisfied if $W_2 T$ is stable and

$$[W_2 GK(I+GK)^{-1}]^* [W_2 GK(I+GK)^{-1}] < 1 \tag{9}$$

for all $\omega \in \Omega$. Note that the argument $e^{j\omega}$ has been omitted for $G(e^{j\omega}), K(e^{j\omega})$ and $W_2(e^{j\omega})$ in order to simplify the notation. Replacing K with XY^{-1} gives:

$$[W_2 GX(Y+GX)^{-1}]^* [W_2 GX(Y+GX)^{-1}] < 1 \tag{10}$$

Multiplying both sides from the right by $(Y + GX)$, and from the left by its complex conjugate, leads to the following matrix inequality:

$$[W_2 GX]^* [W_2 GX] - (Y+GX)^*(Y+GX) < 0 \tag{11}$$

which is a constraint on the difference between two quadratic terms (a convex-concave constraint). In order to convexify the constraint, the second quadratic term is linearized using the following property:

$$P^* P \geq P^* P_c + P_c^* P - P_c^* P_c \tag{12}$$

where $P = Y + GX$ and P_c is any known complex value. We can choose $P_c = Y_c + GX_c$, where $K_c = X_c Y_c^{-1}$ is an initial

controller. Using the Schur complement, the constraint in Eq. 11 can then represented by a linear matrix inequality:

$$\begin{bmatrix} P^*P_c + P_c^*P - P_c^*P_c & (W_2GX)^* \\ W_2GX & 1 \end{bmatrix} > 0 \qquad (13)$$

This convex constraint is a sufficient condition for the spectral constraint in (9) for any choice of $K_c = X_cY_c^{-1}$. However, this constraint will not necessarily represent a convex set of stabilizing controllers. The stability condition will depend on the initial controller K_c and will be discussed in Section 3.3.

3.2 Loop shaping

Assume that a desired open-loop transfer function L_d is available and that the objective is to design a controller K such that the open-loop transfer function $L = GK$ is close to L_d in the 2- or ∞-norm sense. The objective function for the ∞-norm case is to minimize $\|L - L_d\|_\infty$ and can be expressed as follows:

$$\begin{aligned} &\min \gamma \\ &\text{subject to:} \\ &(GK - L_d)^*(GK - L_d) < \gamma \qquad \forall \omega \in \Omega \end{aligned} \qquad (14)$$

Replacing K with XY^{-1} in the constraint, we obtain:

$$(GX - L_dY)^*\gamma^{-1}(GX - L_dY) - Y^*Y < 0 \qquad (15)$$

Again Y^*Y can be linearized around Y_c using the linear approximation in (12). Thus, the following convex formulation is obtained:

$$\begin{aligned} &\min \gamma \\ &\text{subject to:} \\ &\begin{bmatrix} Y^*Y_c + Y_c^*Y - Y_c^*Y_c & (GX - L_dY)^* \\ GX - L_dY & \gamma \end{bmatrix} > 0 \end{aligned} \qquad (16)$$

for all $\omega \in \Omega$.

In a similar way, for minimizing $\|L - L_d\|_2^2$ the following problem can be solved:

$$\begin{aligned} &\min \int_{-\frac{\pi}{T_s}}^{\frac{\pi}{T_s}} \Gamma(\omega) d\omega \\ &\text{subject to:} \\ &(GK - L_d)^*(GK - L_d) < \Gamma(\omega) \qquad \forall \omega \in \Omega \end{aligned} \qquad (17)$$

where $\Gamma(\omega) > 0$ is an unknown function $\in \mathbb{R}$. Replacing K with XY^{-1}, the constraint becomes:

$$(GX - L_dY)^*\Gamma(\omega)^{-1}(GX - L_dY) - Y^*Y < 0 \qquad \forall \omega \in \Omega$$

which results in the following convex optimization problem:

$$\begin{aligned} &\min \int_{-\frac{\pi}{T_s}}^{\frac{\pi}{T_s}} \Gamma(\omega) d\omega \\ &\text{subject to:} \\ &\begin{bmatrix} Y^*Y_c + Y_c^*Y - Y_c^*Y_c & (GX - L_dY)^* \\ GX - L_dY & \Gamma(\omega) \end{bmatrix} > 0 \end{aligned} \qquad (18)$$

for all $\omega \in \Omega$. Note that, in case the constraints are evaluated for a finite set of frequencies $\Omega_N = \{\omega_1, \ldots, \omega_N\}$, $\Gamma(\omega)$ can be replaced with a scalar variable Γ_k at each frequency ω_k.

3.3 Stability analysis

The stability of the closed-loop system is not necessarily guaranteed even if the spectral norm of a weighted sensitivity function is bounded. In fact, every unstable system with no pole on the stability boundary has a bounded spectral norm. In this section, we present the conditions on the linearization of the constraints such that the closed-loop stability can be guaranteed in the following theorem.

Theorem 1. Given a strictly proper plant model G, an initial stabilizing controller $K_c = X_cY_c^{-1}$ with $Y_c \neq 0, \forall \omega \in \Omega$, and feasible solutions X and Y to the following inequality,

$$(Y + GX)^*(Y_c + GX_c) + (Y_c + GX_c)^*(Y + GX) > 0 \qquad (19)$$

for all $\omega \in \Omega$, then the controller $K = XY^{-1}$ stabilizes the closed-loop system if

(1) $Y \neq 0, \forall \omega \in \Omega$.
(2) The initial controller K_c and the final controller K share the same poles on the stability boundary, i.e. $Y = Y_c = 0, \forall \omega \in B_y$

Proof: The proof is based on the Nyquist stability criterion and is given in Karimi and Kammer (2016).

Remark: A necessary and sufficient condition for $Y \neq 0$ is $Y^*Y > 0$. Since this constraint is concave, it can be linearized to obtain the following sufficient convex constraint:

$$Y^*Y_c + Y_c^*Y - Y_c^*Y_c > 0 \qquad (20)$$

For the loop-shaping problems in (16) and in (18), this condition is already included in the formulation. In this case, for guaranteeing the closed-loop stability, only the condition in (19) must be added. This condition can be added directly, or by considering an additional H_∞ constraint on any closed-loop sensitivity function.

4. CONTROLLER DESIGN

The optimization problem described in the previous sections is now used to design a fixed-order SISO controller for an AFM based on frequency-domain data. Some practical issues for designing data-driven controllers are discussed, and the control problem is formulated. The standard control approach in AFM consists of a PI-controller in series with a low-pass filter, where the controller gains are manually tuned by the operator. Using this approach, the main limitation of a scanner's control bandwidth is the excitation of its first mechanical resonance by the scanner drive signal. Too large controller gains degrade the reference tracking performance and introduce ringing, which introduces visible ripples in the AFM image.

We will design a 10th-order controller based on frequency domain data with the goal of providing good tracking performance of the reference for a given bandwidth. The additional degrees of freedom of the controller make it possible to sufficiently dampen the resonance peaks and achieve a good response.

4.1 Plant Identification

The scanner dynamics of a commercial tube scanner (MultiMode JV, Bruker Santa Barbara) have been identified in constant deflection mode. The input of the plant corresponds to the vertical position of the sample, and the output corresponds to the deflection of the cantilever. Both signals are within a range of ± 10 V. The transfer function of the plant is identified by applying 100 periods of a

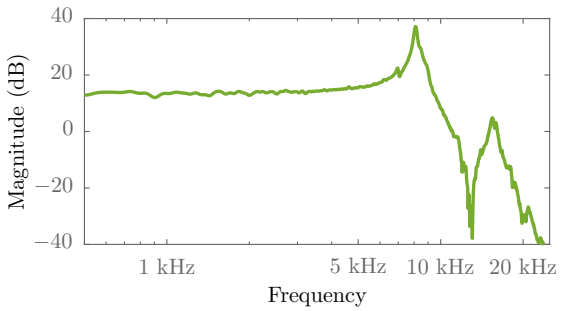

Fig. 1. Frequency response data of the plant G.

pseudorandom binary sequence (PRBS) with a length of 8191 samples and a sampling frequency of 50 kHz. The frequency response is calculated in Matlab using the *spa* command with a Hann window length of 700 and is shown in Fig. 1. One can clearly see the 30 dB resonance peak at around 8 kHz, which limits the performance of the standard PI-controller.

4.2 Constraint Formulation

The objective is to achieve good tracking performance of the reference input with a desired closed-loop bandwidth of 8 kHz. Therefore, as objective function we choose to minimize the 2-norm $\|L - L_d\|_2^2$ between the actual open-loop transfer function L and a desired open-loop transfer function L_d with:

$$L_d = \frac{8 \cdot 10^3 \cdot 2\pi}{s} \tag{21}$$

To improve the robustness, H_∞ constraints on the sensitivity S and closed-loop sensitivity T are introduced. Additionally, the input is constrained to a maximum of 10 V. Therefore, an H_∞ constraint on the input sensitivity U is added.

$$\|W_1 S\|_\infty < 1 \quad ; \quad \|W_2 T\|_\infty < 1 \quad ; \quad \|W_3 U\|_\infty < 1 \tag{22}$$

where $W_1 = 0.4$, $W_3 = 0.1$ and

$$W_2 = \frac{0.1526z^2 + 0.3052z + 0.1526}{z^2 - 0.671z + 0.2523} \tag{23}$$

The values of W_1 and W_3 are chosen based on a worst-case step output disturbance of 1 V. W_2 serves to limit the overshoot to 5 % and adds a roll-off at frequencies above 8 kHz in order to eliminate ringing in the closed-loop response. Note that since the constraints are in frequency domain, the desired L_d and the weighting filters can be in continuous-time, while the designed controller is in discrete-time.

4.3 Initial controller

The stability condition presented in Theorem 1 requires a stabilizing initial controller K_c with the same poles on the stability boundary (the unit circle) as the desired final controller. For a stable plant, a stabilizing initial controller can always be found by choosing:

$$[x_{c,1}, \ldots, x_{c,p}] = 0, \quad x_{c,0} = \epsilon \tag{24}$$

with ϵ being a sufficiently small number. Furthermore, the parameters of:

$$Y_c(z) = (z^p + \cdots + y_{c,1}z + y_{c,0}) \cdot F_y \tag{25}$$

should be chosen such that $Y_c \neq 0$ for all $\omega \in \Omega \backslash B_y$. This can be achieved e.g. by choosing Y_c such that all roots of $Y_c = 0$ lie at zero, with F_y containing all the poles on the unit circle of the desired final controller.

A controller of order $p = 10$ is chosen for this design. Additionally, the controller should contain an integrator, which leads to the following fixed terms:

$$F_x(z) = 1 \qquad F_y(z) = (z - 1)$$

Since the plant is stable, as discussed above the initial controller is found by setting the poles of the controller to 0 and choosing a small enough gain, resulting in the following initial values:

$$X_c(z) = 0.001 \qquad Y_c(z) = z^{10}(z - 1)$$

4.4 Frequency gridding

The optimization problem formulated in the previous section contains an infinite number of constraints (i.e. $\forall \omega \in \Omega$) and is called a semi-infinite problem. A common approach to handle this type of constraints is to choose a large set of frequency samples $\Omega_N = \{\omega_1, \ldots, \omega_N\}$ with $\omega_1 \geq 0$, $\omega_N = \pi/T_s$, and replace the constraints with a finite set of constraints at each of the given frequencies. As the complexity of the problem scales linearly with the number of constraints, N can be chosen relatively large without severely impacting the solver time. Since all constraints are applied to Hermitian matrices, the constraints for the negative frequencies between $-\pi/T_s$ and zero will be automatically satisfied. In some applications with low-damped resonance frequencies, the density of the frequency points can be increased around the resonant frequencies. An alternative is to use a randomized approach for the choice of the frequencies at which the constraints are evaluated (see Alamo et al. (2010)).

The optimization problem is therefore sampled using $N = 1000$ logarithmically spaced frequency points in the interval $\Omega_N = \left[4 \cdot 10^3, 5 \cdot 10^4 \pi\right]$ Hz (the upper limit being the Nyquist frequency of the controller). The lower limit is chosen greater than zero in order to guarantee the boundedness of $L - L_d$.

The constraint sets are formulated for each of the N frequency points. The optimization variable $\Gamma(\omega)$ is replaced by N sampled variables $\Gamma_k, k = 1, \ldots, N$. This results in the following sampled, convex optimization problem :

$$\min_{X,Y} \sum_{k=1}^{N} \Gamma_k \tag{26}$$

subject to:

$$\begin{bmatrix} Y^*Y_c + Y_c^*Y - Y_c^*Y_c & (GX - L_dY)^* \\ GX - L_dY & \Gamma_k \end{bmatrix}(j\omega_k) > 0$$

$$\begin{bmatrix} P^*P_c + P_c^*P - P_c^*P_c & (W_1Y)^* \\ W_1Y & 1 \end{bmatrix}(j\omega_k) > 0$$

$$\begin{bmatrix} P^*P_c + P_c^*P - P_c^*P_c & (W_2GX)^* \\ W_2GX & 1 \end{bmatrix}(j\omega_k) > 0$$

$$\begin{bmatrix} P^*P_c + P_c^*P - P_c^*P_c & (W_3X)^* \\ W_3X & 1 \end{bmatrix}(j\omega_k) > 0$$

$k = 1, \ldots, N$

where the argument $(j\omega_k)$ denotes a constraint evaluated at frequency ω_k, with $P = Y + GX$ and $P_c = Y_c + GX_c$.

4.5 Iterative algorithm

Any LMI solver can be used to solve this optimization problem and calculate a suboptimal controller K around the initial controller K_c. As we only solve an inner convex approximation of the original optimization problem, K depends heavily on the initial controller K_c and the performance criterion can be quite far from the optimal value. The solution is to use an iterative approach that solves the optimization problem multiple times, using the final controller K of the previous step as the new initial controller K_c. This choice always guarantees closed-loop stability (assuming the initial choice of K_c is stabilizing). As the objective function is non-negative and non-increasing, the iteration converges to a local optimal solution of the original non-convex problem (see Yuille and Rangarajan (2003)). The iterative process can be stopped once the change in the performance criterion is sufficiently small.

5. EXPERIMENTAL RESULTS

The optimization problem is formulated in Matlab using Yalmip (see Löfberg (2004)), and solved with Mosek (see MOSEK ApS (2015)). The iteration converges to a final controller in 8 steps, which takes a few minutes on a standard desktop computer in our simple implementation. The bode plot of the final controller K is shown in Fig. 2a. The plot illustrates nicely how the controller compensates the resonance peaks of the plant. The corresponding bode plot of T based on the identified model is given in Fig. 2b and shows that the desired bandwidth is achieved, and that the constraint is satisfied.

In order to validate the results, the controller is implemented in Labview and applied on the real system. Imaging is performed using a home-built high-speed AFM head (see Adams et al. (2014)) using a Bruker FastScan-C cantilever. As the controller runs on an FPGA, the computation time increases only linearly with the controller order, and is negligible in the shown example. The calculations are performed using a fixed-point arithmetic, therefore the controller parameters should be scaled appropriately to achieve a sufficient range and precision. To improve numerical stability and computation speed, the controller can also be broken down into second-order sections. Any in- and output delays are already accounted for in the frequency response of the plant. For high-speed applications it might also be of interest to consider the computation delay in the performance specifications.

The closed-loop response is swept using a lock-in amplifier and is shown in Fig. 2c. One can see that the real response is flat up to the desired bandwidth of 8 kHz, and exhibits the desired roll-off at higher frequencies. The design constraint is almost always satisfied, with an acceptable violation at 16 kHz that does not notably impact the performance. The plot also shows the swept response of the original PI controller. It can be seen how the first resonance peak limits the bandwidth of this controller to 1.2 kHz, and introduces undesired ringing in the response.

Finally, freshly cleaved mica was lightly sanded with 8um grit lapping film to create terraced trenches. The sample surface was imaged at a line rate of 57 Hz and a surface

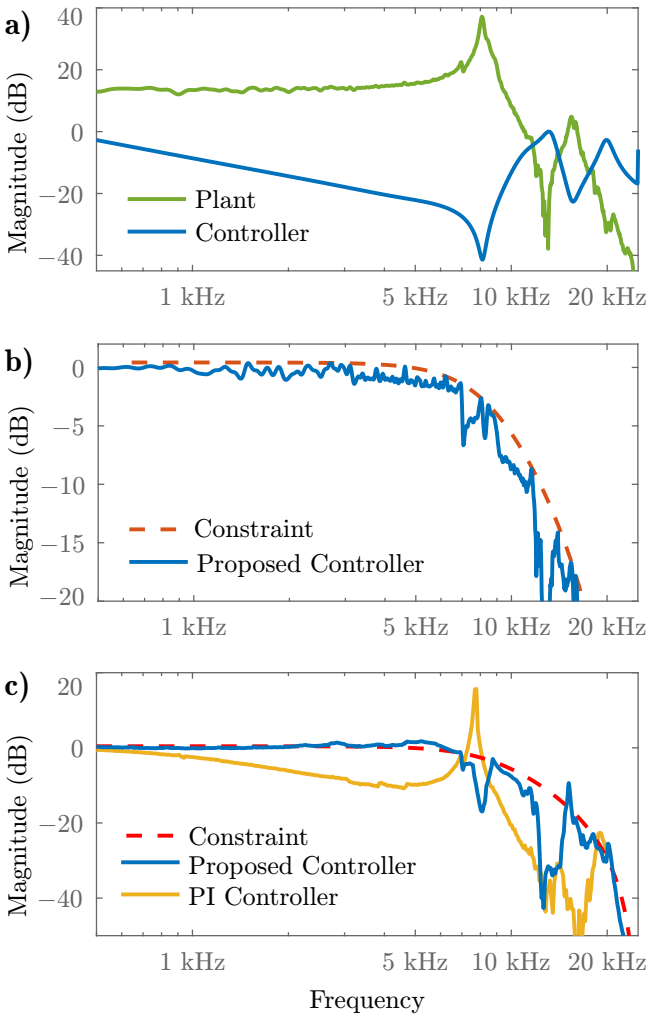

Fig. 2. Bode magnitude plots of: a) Controller K. b) Expected closed-loop sensitivity T. c) Measured closed-loop sensitivity T of the proposed controller (blue), outperforming a conventional PI controller (yellow) by an order of magnitude.

speed of 912 μm/s, which is about 10 times faster than the conventional approach. Imaging was performed in constant deflection mode with a setpoint of 25 nm. The images of the topography and the error shown in Fig. 3 illustrate the excellent step tracking of the controller at this speed.

6. CONCLUSION

We have presented a novel method to design data-driven, fixed-structure controllers using convex optimization. The method was applied on an atomic-force microscope to significantly increase the imaging bandwidth and reduce the time needed to capture an image by one order of magnitude. Once an optimal controller has been computed for a given system, it can also be used as near-optimal initial controller in future tuning sessions. This allows the iteration to converge quickly to a new optimal controller and greatly reduces the computation time. This is a significant reduction compared to the conventional method of manually tuning the controller parameters which, combined

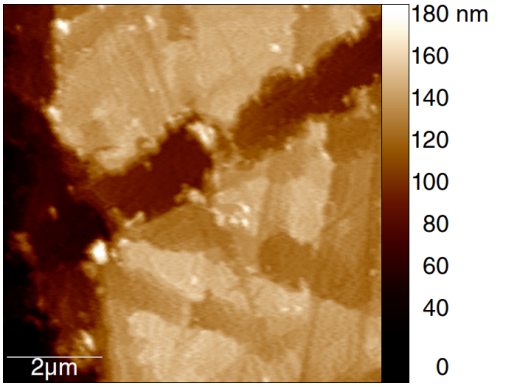

(a)

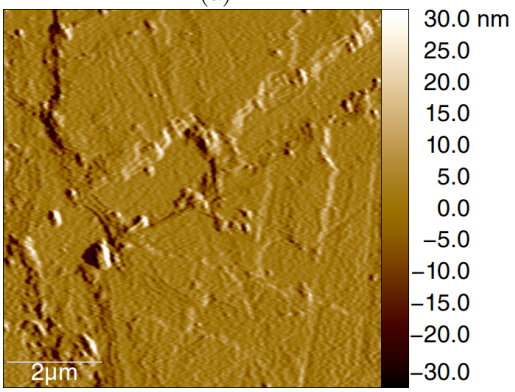

(b)

Fig. 3. Atomic force microscopy imaging of a sanded muscovite mica surface at 57 lines/second (912um/s surface speed) with the proposed controller. a) Topography image showing clear sharp edges and no parachuting artifacts or scanner ringing. b) Corresponding recording of the controller error.

with the guarantee of stability and performance, makes the presented method well suited for this application.

REFERENCES

Adams, J.D., Nievergelt, A., Erickson, B.W., Yang, C., Dukic, M., and Fantner, G.E. (2014). High-speed imaging upgrade for a standard sample scanning atomic force microscope using small cantilevers. *Review of Scientific Instruments*, 85(9), 093702.

Alamo, T., Tempo, R., and Luque, A. (2010). On the sample complexity of probabilistic analysis and design methods. In *Perspectives in Mathematical System Theory, Control, and Signal Processing*, 39–55. Springer.

Ando, T. (2008). Control techniques in high-speed atomic force microscopy. In *American Control Conference, 2008*, 3194–3200. IEEE.

Boyd, S., Hast, M., and Åström, K.J. (2016). MIMO PID tuning via iterated LMI restriction. *International Journal of Robust and Nonlinear Control*, 26(8), 1718–1731.

Fantner, G.E., Schitter, G., Kindt, J.H., Ivanov, T., Ivanova, K., Patel, R., Holten-Andersen, N., Adams, J., Thurner, P.J., Rangelow, I.W., et al. (2006). Components for high speed atomic force microscopy. *Ultramicroscopy*, 106(8), 881–887.

Galdos, G., Karimi, A., and Longchamp, R. (2010). H_∞ controller design for spectral MIMO models by convex optimization. *Journal of Process Control*, 20(10), 1175 – 1182.

Hast, M., Aström, K.J., Bernhardsson, B., and Boyd, S. (2013). PID design by convex-concave optimization. In *European Control Conference*, 4460–4465. Zurich, Switzerland.

Karimi, A. and Galdos, G. (2010). Fixed-order H_∞ controller design for nonparametric models by convex optimization. *Automatica*, 46(8), 1388–1394.

Karimi, A. and Kammer, C. (2016). A data-driven approach to robust control of multivariable systems by convex optimization. *arXiv:1610.08776 [math.OC]*.

Karimi, A., Kunze, M., and Longchamp, R. (2007). Robust controller design by linear programming with application to a double-axis positioning system. *Control Engineering Practice*, 15(2), 197–208.

Karimi, A., Nicoletti, A., and Zhu, Y. (2016). Robust H_∞ controller design using frequency-domain data via convex optimization. *available online in International Journal of Robust and Nonlinear Control*.

Keel, L.H. and Bhattacharyya, S.P. (2008). Controller synthesis free of analytical models: Three term controllers. *IEEE Trans. on Automatic Control*, 53(6), 1353–1369.

Löfberg, J. (2004). YALMIP: A toolbox for modeling and optimization in MATLAB. In *CACSD Conference*. `http://control.ee.ethz.ch/joloef/yalmip.php`.

Mercader, P., Åström, K.J., T., A.B., and Hägglund (2016). Robust PID design based on QFT and convex-concave optimization. *IEEE Trans. in Control Systems Technology*.

MOSEK ApS (2015). *The MOSEK optimization toolbox for MATLAB manual. Version 7.1.* URL `http://docs.mosek.com/7.1/toolbox/index.html`.

Nievergelt, A.P., Erickson, B.W., Hosseini, N., Adams, J.D., and Fantner, G.E. (2015). Studying biological membranes with extended range high-speed atomic force microscopy. *Scientific reports*, 5.

Parastvand, H. and Khosrowjerdi, M.J. (2015). Controller synthesis free of analytical model: fixed-order controllers. *Int. Journal of Systems Science*, 46(7), 1208–1221.

Parastvand, H. and Khosrowjerdi, M.J. (2016). Parameterised controller synthesis for SISO-LTI uncertain plants using frequency domain information. *International Journal of Systems Science*, 47(1), 32–44.

Saeki, M. (2014). Data-driven loop-shaping design of PID controllers for stable plants. *International Journal of Adaptive Control and Signal Processing*, 28(12), 1325–1340.

Saeki, M., Ogawa, M., and Wada, N. (2010). Low-order H_∞ controller design on the frequency domain by partial optimization. *International Journal of Robust and Nonlinear Control*, 20(3), 323–333.

Schitter, G., Allgöwer, F., and Stemmer, A. (2003). A new control strategy for high-speed atomic force microscopy. *Nanotechnology*, 15(1), 108.

Yuille, A.L. and Rangarajan, A. (2003). The concave-convex procedure. *Neural Computation*, 15(4), 915–936.